

УДК 552.11+551.22

© L. P. NIKITINA, *•** M. S. BABUSHKINA, * A. G. GONCHAROV*•**

**GEOCHEMISTRY OF REE AND HFSE IN THE
MANTLE PERIDOTITE AND PYROXENITE XENOLITHS
FROM QUATERNARY VOLCANOES OF NORTH-WEST SPITSBERGEN**

* Institute of Precambrian Geology and Geochronology RAS, Makarova emb., 2,
Saint Petersburg, 199034, Russia

** Institute of Earth Sciences, Saint Petersburg State University, Universitetskaya emb., 7—9,
Saint Petersburg, 199034, Russia; e-mail: lpnikitina2011@yandex.ru

This paper presents new data on geochemistry of rare-earth and high-field-strength elements in the upper mantle peridotite (spinel lherzolites) and pyroxenite (amphibole clinopyroxenites, garnet clinopyroxenites, websterites, and garnet websterites) xenoliths collected from Quaternary volcanoes of the north-western part of Spitsbergen Island, Svalbard Archipelago. The fractionating of HFSE in the peridotites and pyroxenites, and the effect of temperature on the equilibration distribution of these elements between minerals of spinel lherzolites have been investigated based on geochemical features of rocks and minerals, obtained by ICP MS and SIMS. It has been concluded that fractionation of Nb, Ta, Zr, Hf, and Ti occurs in the upper part of the continental lithospheric mantle under the conditions that exist at depth corresponding to the Moho discontinuity (at the temperature from 730 to 1180 °C and pressures from 1.3 to 2.7 GPa). These conditions correspond to those of the phase transition of spinel peridotites into garnet peridotites in the CMAS systems. It is most likely that the degree of partial melting and the thermodynamic conditions of this process are the main factors regulating fractionation of HFSE. The fractionation of these elements in the mantle of north-west Spitsbergen is noticeably different than in the mantle beneath Early Precambrian cratons.

Key words: xenoliths, peridotites and pyroxenites, upper mantle, REE, HFSE, fractionation.

Д. чл. Л. П. НИКИТИНА, *, ** д. чл. М. С. БАБУШКИНА, * А. Г. ГОНЧАРОВ*, **
ГЕОХИМИЯ REE И HFSE В КСЕНОЛИТАХ ВЕРХНЕМАНТИЙНЫХ
ПЕРИДОТИТОВ И ПИРОКСЕНИТОВ ИЗ ЧЕТВЕРТИЧНЫХ БАЗАЛЬТОВ
СЕВЕРО-ЗАПАДНОГО ШПИЦБЕРГЕНА

* Институт геологии и геохронологии докембрия РАН
** Санкт-Петербургский государственный университет

В статье приводятся новые данные по геохимии редкоземельных (REE) и высокозарядных (HFSE) элементов для верхнемантийных ксенолитов из четвертичных базальтов северо-западного Шпицбергена, относящихся к породам перидотитовой (шпинелевые лерцолиты) и пироксенитовой (амфиболовые и гранатовые клинопироксениты, гранатовые и безгранатовые вебстериты) серий. На основе данных о содержании элементов в валовых пробах и минералах, полученных методами ICP MS и SIMS, исследовано фракционирование HFSE в перидотитах и пироксенитах, а также влияние температуры на равновесное распределение этих элементов между минералами шпинелевых лерцолитов. Показано, что фракционирование Nb, Ta, Zr, Hf и

Ti происходило в верхней части континентальной литосферной мантии в условиях близких к тем, которые имеют место на границе Мохо (в интервале температур и давлений 730—1180 °C, 1.3—2.7 ГПа соответственно). Эти условия соответствуют границе между двумя фациями глубинности (шпинелевых перидотитов и гранатовых перидотитов). Наряду с термодинамическими параметрами, фактором фракционирования выступала степень плавления мантийного субстрата. Сделан вывод о том, что фракционирование HFSE в верхней мантии, подстилающей северо-западный Шпицберген, протекало существенно иначе, чем в мантии, расположенной под раннедокембрийскими кратонами.

Ключевые слова: ксенолиты, перидотиты, пироксениты, верхняя мантия, редкоземельные и высокозарядные элементы, фракционирование.

INTRODUCTION

This paper presents new data on geochemistry of rare-earth elements (REE) and high field-strength elements (HFSE) in the mantle peridotite and pyroxenite xenoliths collected from Quaternary volcanoes of the north-western part of Spitsbergen Island, Svalbard archipelago. The effect of temperature on the equilibration distribution of HFSE between the minerals of spinel peridotites, covering the temperature range of 730 to 1180 °C and pressure from 1.3 to 2.7 GPa, as well as the fractionating of HFSE in peridotites and pyroxenites in the shallow mantle near Moho have been investigated based on geochemical features of Svalbard xenoliths.

Geochemical studies of HFSE in mantle rocks and minerals are the leading topic of modern mantle research. Because these elements are geochemical indicators of the crust-mantle interaction, they help to identify sources of magmatic derivatives. Recent studies have revealed that a mass imbalance exists for Nb, Ta and possibly Ti in the Earth: the continental crust and depleted mantle both have sub-chondritic Nb/Ta, Nb/La and Ti/Zr ratios (Barth et al., 2000; Rudnick et al., 2000; Münker et al., 2003; Weyer et al., 2003; Pfänder et al., 2007; König, Schuth, 2011). The Nb/Ta ratio of the silicate Earth is approximately 14.0. In the crust, this ratio is equal to 12.0—13.0. In the basalts of the mid-ocean ridges, the average value of this ratio is 14.6, whereas in the chondrite C1 it is equal to 17.4—17.6. The continental crust and the depleted mantle are not strictly complementary in their Nb relation, and no mixing of these two reservoirs can produce the chondritic Nb/Ta and Nb/La ratios in the silicate Earth. This leads to the assumption that the silicate Earth has lost a certain amount of Nb and that there must be an additional reservoir with a superchondritic Nb/Ta ratio. Thus, it is considered that such reservoir may be subducted into the lower mantle the oceanic crust, transformed into rutile-bearing eclogites at the core-mantle boundary (Rudnick et al., 2000). Another hypothesis has been suggested by Wade and Wood (2001), who proposed that the important role of the global budget of Nb is attributed to the terrestrial core. According to this hypothesis, niobium may be partly dissolved in the core. The experimental studies of the chemical properties of Nb and Ta indicate a change in siderophile properties of Nb at high pressures, and show the lower siderophile character of Ta than Nb, which is similar to that of vanadium (Mann et al., 2009; Wade, Wood, 2001). A number of researchers have indicated the need to examine the role of the continental lithospheric mantle (CLM) in the global budget of Nb (Pfänder et al., 2012). Model calculations reveal that approximately 30 % of Nb may occur in the continental lithospheric mantle, but according to the authors a high Nb/Ta ratio in the mantle is most likely limited to domains that have undergone carbonatite metasomatism. HFSE research on mantle peridotite and eclogite xenoliths (Nikitina, 2013; Nikitina et al., 2014; Nikitina et al., 2015) support a hypothesis about the partial

concentration of the missing niobium in the continental lithospheric mantle. Indeed, the investigations show that the Nb/Ta and Nb/La ratios in mantle peridotite xenoliths, in spite of wide fluctuations (Nb/Ta from 8—10 to 80—100 and Nb/La from 0.5 to 4—5), exceed chondritic values (17.6 and 1.0, respectively). Xenoliths from the mantle beneath the Early Precambrian cratons, e. g., the Kaapvaal craton or cratons of Eastern Siberian and North American platforms, are characterized by highest Nb concentrations (0.15—10 ppm). Some researchers do not accept the fractionation of Nb and Ta, or other HFSE in the upper mantle. Schmidt and co-authors (2009) consider that during the transformation of the oceanic crust into eclogites, Nb, Ta, Zr, Hf, and Ti have, on average, identical mobility, so significant fractionation of Nb and Ta is not manifested.

The variations of Zr/Hf and Nb/Ta ratios in the natural reservoirs have a decisive importance in our understanding of the differentiation of the crust-mantle system. Experimental data and observations show that these ratios change during the magmatic process, in spite of very similar geochemical characteristics of these elements. All basalts, including basalts of Archean greenstone belts, MORB, and OIB, have sub-chondritic Nb/Ta values and Zr/Hf values varying from sub-chondritic to superchondritic (Büchl et al., 2002; Münker et al., 2003; Pfänder et al., 2007).

On this basis, following questions need to be answered: 1. What are the variations of Nb/Ta, Nb/La, Ti/Zr, Zr/Hf ratios in mantle xenoliths relative to those in chondrite? 2. What are the degree and conditions for fractionation of Nb, Ta, Zr, Hf, Ti in the shallow mantle near Moho? In this paper we try to answer to these questions using new geochemical data for mantle xenoliths from Quaternary basalts of north-west Spitsbergen.

Mantle xenoliths (18 samples of peridotites and 14 samples of pyroxenites) were collected from lavas and pyroclastic material of the Sverre Quaternary stratovolcano and of the Sigurd and Halvdan slag cones, that located in the north-western part of Spitsbergen Island along the deep Breibogen Fault (Johansson et al., 2005). The K-Ar ages of the appearance of the Halvdan and Sigurd volcanic cones are 2.7 and 2.0 Ma respectively, the age of the Sverre volcano is between 10 and 6 thousand years (Evdokimov, 2000; Sirokin, Sharin, 2000). The displacement of the focus of Quaternary volcanism from south to north coincides with the opening of the eastern Arctic Basin and the Norwegian-Greenland Sea (Sushchevskaya et al., 2008).

The petrography and mineralogy as well as equilibration conditions (P , T , f_{O_2}) for mineral assemblages observed in the studied xenoliths were described in detail earlier (Glebovitskii et al., 2011; Goncharov et al., 2015). In the cited papers, one can find a survey of previous publications concerned with the composition of mantle xenoliths, metasomatic processes and the upper mantle structure within the region (Amundsen et al., 1987; Genshaft, Ilupin, 1987; Genshaft et al., 1993; Ionov et al., 1993, 1996; Kopylova et al., 1996; Shubina et al., 1997; Maslov, Lasarennkov, 1999; Maslov, 2000; Evdokimov, 2000; Glebovitskii et al., 2011).

ANALYTICAL METHODS

The xenoliths selected for chemical analysis have not been affected by secondary processes such as development of carbonates in peridotites or the formation of fine-grained zones in pyroxenites. They were carefully cut using a diamond saw to remove the basalt rims.

The chemical composition of rocks was determined by XRF (for the major oxides) and ICP-MS (for trace elements such as V, Cr, Co, Ni, Cu, Zn, Rb, Sr, Y, Zr, Nb, Ba, La, Hf, Ta, Pb, Th, U) in the Central Laboratory of Russian Geological Research Institute, Saint Petersburg. For XRF analysis, silicate was mixed with the flux (50 % lithium metaborate and 50 % lithium tetraborate) at 1:9 ratio and smelted in gold-platinum crucibles at the Classe Fluxer-Bis company (Canada). The lower limits of detection for SiO_2 and Al_2O_3 , MgO and Na_2O , and other oxides were 0.02, 0.05, and 0.01 wt %, respectively. The REE contents in a solution of powdered rock samples were determined using a quadrupole mass spectrometer with inductively coupled plasma. The deviation of error in determining Th, U, Pb, Hf, Lu, Yb, Er, and Dy concentrations was estimated to be 10–15 %, the errors for the rest of the trace elements including Ti, Sc, Zr, Sr and Nb were no more than 5 %. The trace element contents in minerals were ascertained using Cameca SIMS-4f ion microprobe (Yaroslavl Branch, Physical Technical Institute, Russian Academy of Sciences) by the method described in (Fedotova et al., 2008).

WHOLE ROCK CHEMISTRY

Studied peridotite xenoliths are spinel lherzolites characterized by the assemblage of olivine (Ol) + orthopyroxene (Opx) + clinopyroxene (Cpx) + spinel (Spl), where Ol abundance is up to 84 %, Opx is up to 29 %, Cpx is up to 15 %, and Spl is up to 4 %. Kaersutite is present as a minor mineral. The modal composition of each xenoliths, calculated by the least-squares method from the whole rock and minerals chemistry, as well as the P – T conditions inferred from mineral equilibria are shown in Table 1. The major and trace element compositions of peridotite xenoliths are presented in Table 2. They are characterized by an Al/Si ratio less than 0.112 (primitive mantle, PM) and an Mg/Si ratio higher than 1.047 (PM). On Al/Si vs. Mg/Si and Ca/Si diagrams (Fig. 1), peridotite xenoliths show approximate linear correlations between the ratios. These trends coincide with those reflected a change of the composition of primitive spinel peridotites INTA and INTB at 1270–1390 °C and 1.0 GPa (Schwab, Johnston, 2001) and garnet peridotite WKR at 1515–1950 °C and 3–7 GPa (Walter, 1998) as a function of the melting degree.

Peridotite xenoliths, according to the primitive mantle-normalized rare-earth element pattern, are depleted relative to PM and show a flat distribution of REE from Sm to Lu (Fig. 2, a). An insignificant increase of Pr, Ce and La was observed for the majority of the samples, including that with $\text{La}_N > 1$. The contents of Nd, Sm, Dy, Er, and Yb monotonically decrease with an increase in the Mg/Si ratio (Fig. 3, a, b). The resultant relations are similar to melting residues from the spinel peridotite INTA at 1 GPa pressure over the temperature range from 1280 °C to 1390 °C (Johnston, Schwab, 2004). However, the contents of these elements in the residues are lower than in peridotite xenoliths at the same Mg/Si ratio.

PM-normalized Rb-Lu patterns (Fig. 2, b) demonstrate a positive anomaly for Nb and negative anomalies for Ta and Ti. Accordingly, peridotites are characterized by the chondritic and predominantly superchondritic Nb/Ta ratio ranging from 14.5 to 100. This ratio in the chondrite is equal to 17.4–17.6 (Barth et al., 2000; Palme, O'Neill, 2003; Rudnick et al., 2004). The Nb/La ratio varies between 0.43 and 5.1, and in the majority of the samples it is lower than the same ratio (1.01) for chondrite C1 (Palme, O'Neill, 2003). The Ti/Zr and Zr/Hf ratios range from

Table 1

Modal compositions and $P-T$ conditions for peridotite xenolithsМодальные составы и $P-T$ условия минеральных равновесий для ксенолитов перидотитов

Sample	Volcano	Modal composition, %				$T, ^\circ C$	P, GPa
		Ol	Opx	Cpx	Spl		
2161-71	III	74	14	10	2	930	1.9
2161-2	III	74	18	6	2	1060	2.4
2166-10	I	59	27	11	3	730	1.3
2166-11	III	83	9	6	2	1030	2.3
2166-16	I	—	—	—	—	940	2
2166-18	I	69	19	9	3	930	2
2166-24	I	60	27	10	3	880	1.8
2166-25	I	67	24	7	2	1150	2.7
2166-26	I	73	19	7	1	790	1.5
2166-3	I	51	33	13	3	910	1.9
2166-6	I	85	4	9	2	940	2
2166-7	I	84	5	10	1	1180	2.7
2166-8	I	79	11	7	3	770	1.5
2166-9	I	63	26	9	2	850	1.7
2172-24	II	82	10	7	1	1090	2.5
CB-51	I	63	27	8	2	960	2.1
Sp-2	III	62	27	10	1	950	2
Sp-28	III	62	21	15	2	1080	2.4

Notes. Volcano: I - Sverre, II - Halvdan, III — Sigurd. Temperature calculated with the Opx-Cpx thermometer of Wood and Banno (1973), pressure calculated by projection of temperature estimates to the 55 mW/m² regional geotherm of Hasterok and Chapman (2011). The modal compositions of xenoliths calculated by the least-squares method using the whole-rock and mineral chemistry.

19.1 to 154.6 for the former and from 28.4 to 52.4 for the latter. In most cases they are lower and higher respectively, than in the chondrite C1 (Ti/Zr 119.6, Zr/Hf 36.1).

In Fig. 4, the variations of the HFS element concentrations and their ratios for studied xenoliths are plotted. Here, the compositions of spinel peridotite xenoliths in Quaternary basalts from different regions are also shown for comparison. The significant spread of the HFSE ratios is observed within all diagrams. Only peridotites from the mantle of the Central Asian Belt (Tokinsky Stanovik and Mongolia) form the separate field on the diagram of Zr/Hf vs Zr. These peridotites are characterized by high contents of Hf (higher than in the chondrite C1, where the Hf content is 3.86 ppm) and superchondritic values of Zr/Hf.

Pyroxenite xenoliths were collected from basalts of the Sigurd volcano. Their modal compositions and $P-T$ conditions are shown in Table 3. Whole-rock major- and trace-element contents are summarized in Table 4. These xenoliths are characterized by the Al/Si, Ca/Si ratios higher and the Mg/Si ratio lower than in primitive mantle (Fig. 1). The Mg/Si ratio for studied xenoliths does not change substantially, while the Al/Si ratio varies from 0.15 to 0.55. The pyroxenite xenoliths form trends that intersect the PM geochemical fractionation line (Fig. 1) and also intersect trends of melts composition, which formed during the melting of the primitive spinel peridotites (Schwab, Johnston, 2001) and the garnet peridotite (Walter,

Table 2

Химический состав ксенолитов шинелевых перидотитов Шпицбергена
Compositions of spinel peridotite xenoliths (major oxides in wt%, trace elements in ppm)

Sample Volcano	2166-3 1	2166-6 1	2166-7 1	2166-8 1	2166-9 1	2166-10 1	2166-18 1	2166-25 1	2166-26 1	CB-51 1	CB-67 1	2172-24 1	2166-24 1	2166-11 III	2161-71 III	2162-2 III	Sp-2 III	Sp-28 III
SiO ₂	44.50	41.50	41.70	42.80	43.40	44.60	43.00	43.90	43.80	44.60	44.80	42.50	44.50	43.00	42.60	43.00	45.10	43.90
TiO ₂	0.13	0.12	0.05	0.07	0.08	0.12	0.11	0.09	0.01	0.06	0.01	0.03	0.07	0.06	0.04	0.02	0.03	0.11
Al ₂ O ₃	3.56	1.82	1.54	2.51	2.59	3.30	2.97	2.20	1.45	2.29	1.68	1.54	3.18	1.72	2.73	1.55	2.55	3.30
FeO	8.14	8.21	8.20	7.70	8.05	7.88	7.62	8.24	7.50	8.23	7.51	8.05	7.81	8.08	7.97	8.50	7.95	8.32
MnO	0.13	0.12	0.12	0.12	0.12	0.13	0.12	0.13	0.12	0.12	0.12	0.12	0.12	0.12	0.12	0.13	0.13	0.13
MgO	37.20	44.50	44.90	42.80	40.20	39.90	42.20	42.30	44.00	41.60	43.40	45.10	40.50	44.00	42.80	43.50	40.60	39.40
CaO	3.00	2.13	1.97	1.76	2.07	2.71	2.20	1.66	1.79	2.02	1.62	1.49	2.38	1.35	2.35	1.85	2.38	3.29
Na ₂ O	0.35	<0.05	<0.05	0.25	0.19	0.18	0.11	0.10	0.11	0.25	0.16	0.14	0.17	<0.05	0.21	<0.05	0.18	0.30
K ₂ O	0.08	0.10	0.08	0.06	0.08	0.06	0.06	0.06	0.06	0.14	0.18	0.14	0.13	0.06	0.05	0.14	0.14	0.15
P ₂ O ₅	<0.05	<0.05	<0.05	<0.05	<0.05	<0.05	<0.05	<0.05	<0.05	<0.05	<0.05	<0.05	<0.05	<0.05	<0.05	<0.05	<0.05	<0.05
LOI	1.59	<0.1	<0.1	0.57	1.84	<0.1	0.27	<0.1	<0.1	<0.1	<0.1	<0.1	<0.1	<0.1	0.31	<0.1	<0.1	<0.1
Total	95.5	98.5	98.6	97.5	94.9	98.9	98.1	98.7	98.9	99.4	99.1	98.8	98.1	99.0	98.8	99.1	98.9	98.9
V	<5.0	47	72	<5.0	5.8	<5.0	<5.0	5.2	48	50	45	<5.0	<5.0	<5.0	54.9	44	67	74
Cr	1950	1629	1361	2020	2050	2150	2020	2010	2160	1120	1640	1370	2110	2010	1930	1106	1640	2130
Co	n.d.	98	103	n.d.	n.d.	n.d.	n.d.	n.d.	n.d.	112	103	101	120	n.d.	n.d.	123	95	119
Ni	n.d.	1410	1475	n.d.	n.d.	n.d.	n.d.	n.d.	n.d.	1110	877	1030	1140	n.d.	n.d.	1200	1345	1130
Rb	1.18	0.21	0.11	0.73	1.25	0.67	0.87	0.79	<2	n.d.	<2	0.88	1.10	<2	0.58	n.d.	n.d.	n.d.
Sr	13.50	19.46	10.45	8.93	14.50	7.35	13.90	18.30	6.93	35.70	n.d.	23.90	11.20	8.98	25.00	37.64	n.d.	n.d.
Y	3.18	2.22	1.47	1.71	2.02	2.77	2.44	1.64	0.82	1.90	n.d.	1.11	2.29	1.54	0.76	1.44	n.d.	n.d.
Zr	10.40	4.65	2.11	1.33	9.47	6.18	7.94	7.11	3.14	5.12	n.d.	5.04	4.19	4.61	3.51	1.34	n.d.	n.d.
Nb	0.74	0.35	0.03	1.53	1.20	<0.5	<0.5	0.75	<0.5	n.d.	<0.5	n.d.	0.53	<0.5	0.58	1.00	n.d.	n.d.
Cs	0.12	0.06	0.04	0.11	0.13	0.09	0.12	0.12	<0.1	n.d.	<0.1	n.d.	<0.1	0.09	0.19	<0.1	0.05	n.d.
Ba	6.20	6.55	1.28	<3.0	<3.0	7.30	6.30	10.00	<3	4.44	n.d.	5.28	6.70	13.10	<3	18.85	n.d.	n.d.
Hf	0.28	0.16	0.06	0.07	0.26	0.21	0.22	0.18	0.08	0.18	n.d.	0.12	0.10	0.07	0.03	n.d.	n.d.	n.d.
Ta	0.04	0.02	<0.01	0.02	0.02	<0.01	0.01	<0.01	<0.01	n.d.	<0.01	n.d.	<0.01	0.01	0.01	0.04	0.01	n.d.

Table 2 (continued)

	Sample Volcano	2166-3	2166-6	2166-7	2166-8	2166-9	2166-10	2166-18	2166-25	2166-26	CB-51	CB-67	2172-24	2166-24	2166-11	2161-71	2162-2	Sp-2	Sp-28
Th	0.11	0.10	0.01	0.06	0.17	0.05	0.08	<0.1	0.16	n.d.	<0.1	0.10	0.06	<0.1	0.14	n.d.	n.d.	n.d.	
U	0.06	0.05	0.01	<0.05	0.09	<0.05	0.06	<0.05	0.21	n.d.	<0.05	0.06	0.06	<0.1	0.02	n.d.	n.d.	n.d.	
La	0.68	0.81	0.12	0.30	0.86	0.28	0.59	1.04	0.19	2.52	n.d.	0.67	0.57	0.38	0.14	1.14	n.d.	n.d.	
Ce	1.37	1.25	0.18	0.68	1.74	0.66	1.00	1.74	0.45	5.84	n.d.	1.52	0.82	0.76	0.49	3.33	n.d.	n.d.	
Pr	0.20	0.10	0.01	0.09	0.22	0.12	0.13	0.20	0.05	0.60	n.d.	0.20	0.08	0.13	0.09	n.d.	n.d.	n.d.	
Nd	0.93	0.74	0.25	0.44	0.90	0.66	0.60	0.78	0.13	2.19	n.d.	0.86	0.36	0.52	0.40	2.54	n.d.	n.d.	
Sm	0.27	0.25	0.11	0.15	0.24	0.21	0.19	0.19	0.05	0.26	n.d.	0.13	0.15	0.18	0.17	0.39	n.d.	n.d.	
Eu	0.11	0.08	0.03	0.05	0.07	0.09	0.07	0.07	0.04	0.05	n.d.	0.05	0.05	0.04	0.07	0.10	n.d.	n.d.	
Gd	0.35	0.27	0.20	0.20	0.24	0.29	0.28	0.22	0.04	0.27	n.d.	0.12	0.18	0.17	0.21	0.42	n.d.	n.d.	
Tb	0.07	0.07	0.04	0.04	0.04	0.06	0.06	0.04	0.01	0.04	n.d.	0.03	0.04	0.04	0.04	0.05	n.d.	n.d.	
Dy	0.47	0.30	0.33	0.27	0.32	0.41	0.37	0.27	0.09	0.33	n.d.	0.20	0.29	0.20	0.25	0.32	n.d.	n.d.	
Ho	0.10	0.07	0.06	0.08	0.10	0.09	0.06	0.04	0.04	0.08	n.d.	0.05	0.08	0.06	0.05	n.d.	n.d.	n.d.	
Er	0.32	0.19	0.13	0.17	0.22	0.26	0.27	0.17	0.02	0.16	n.d.	0.15	0.24	0.14	0.22	0.21	n.d.	n.d.	
Tm	0.05	0.07	0.03	0.03	0.05	0.03	0.02	0.01	0.05	n.d.	0.03	0.04	0.03	0.03	0.02	n.d.	n.d.	n.d.	
Yb	0.37	0.28	0.22	0.17	0.23	0.25	0.25	0.17	0.10	0.13	n.d.	0.16	0.27	0.16	0.10	0.12	n.d.	n.d.	
Lu	0.06	0.03	0.03	0.02	0.03	0.04	0.04	0.04	0.02	0.05	n.d.	0.03	0.04	0.03	0.05	0.04	n.d.	n.d.	
Mg/Si	1.079	1.384	1.390	1.291	1.196	1.155	1.267	1.244	1.297	1.204	1.251	1.370	1.175	1.321	1.297	1.306	1.162	1.159	
Nb/Ta	18.5	17.5	—	76.5	60.0	—	—	75.0	—	—	—	53.0	—	14.5	100	—	—	—	
Nb/La	1.09	0.43	0.25	5.10	1.40	—	—	0.72	—	—	—	0.93	—	4.14	0.88	—	—	—	
Ti/Zr	74.88	154.58	141.94	31.53	50.60	116.31	82.98	75.82	19.08	70.20	—	35.65	100.07	77.96	71.33	89.40	—	—	
Zr/Hf	37.14	29.06	35.17	19.00	36.42	29.43	36.09	39.50	39.25	28.44	—	42.00	34.92	46.10	52.39	44.67	—	—	

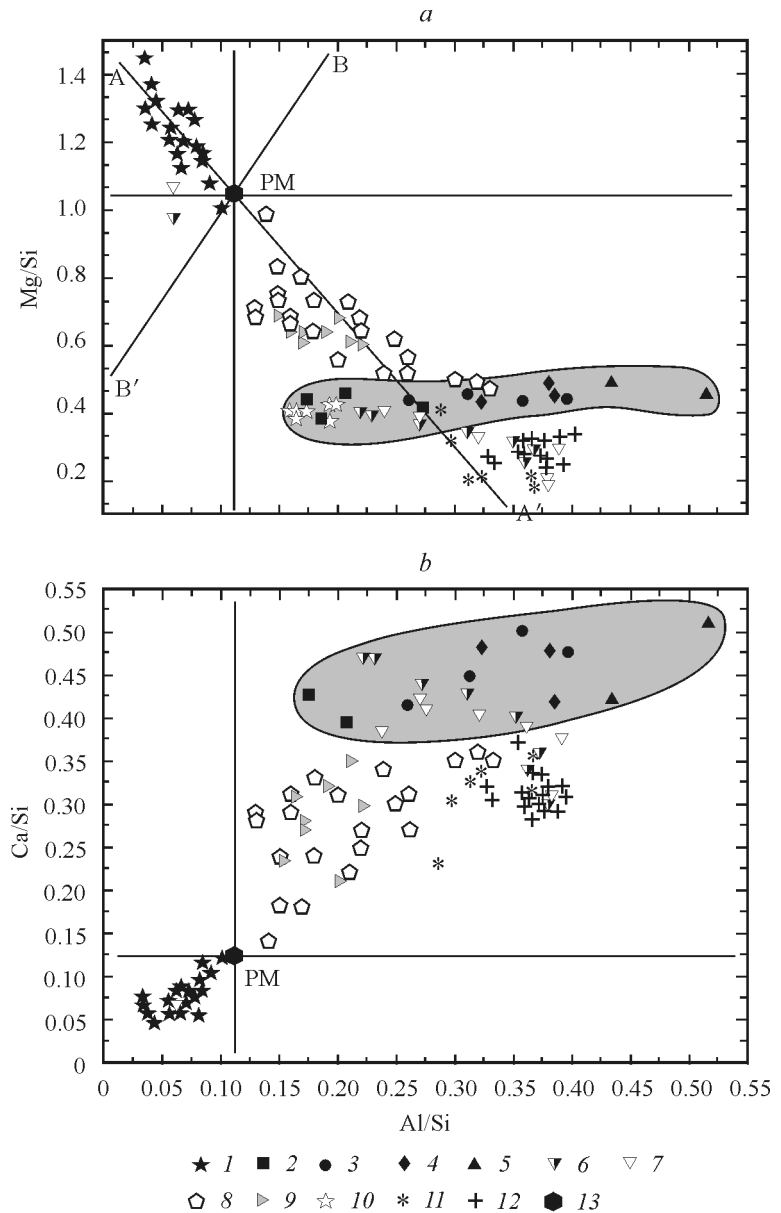


Fig. 1. Al-Si vs Mg/Si (a) and Ca/Si (b) diagrams for mantle xenoliths and partial melts formed in mantle peridotites. For reference, average compositions of basaltic rocks are also plotted.

1—5 — xenoliths (1 — peridotites, 2—5 — pyroxenites: 2 — websterites, 3 — garnet websterites, 4 — garnet clinopyroxenites, 5 — amphibole-bearing garnet clinopyroxenites); 6—8 — melts, formed during melting of INTA (6) and INTB (7) spinel peridotites at 1270—1390 °C and 1.0 GPa (Schwab, Johnston, 2001) and WKR garnet peridotite (8) formed at 1515—1690 °C and 3—7 GPa (Walter, 1998); 9 — picrites (Zhang et al., 2008), 10 — MORB (Klein, 2003); 11 — alkaline basalts (Farmer, 2007); 12 — Quaternary alkaline olivine basalts of NW Spitsbergen (Evdokimov, 2000); 13 — PM (Plame, O'Neill, 2003). Lines A—A' and B—B' show, respectively, trends of geochemical and cosmochemical fractionation from Jagoutz et al (1979). Shaded areas outline fields of the studied pyroxenite compositions.

Рис. 1. Вариации содержаний главных компонентов в мантийных ксенолитах и расплавах, образовавшихся при плавлении перидотитов. Для сравнения на диаграмму вынесены средние составы базальтовых пород.

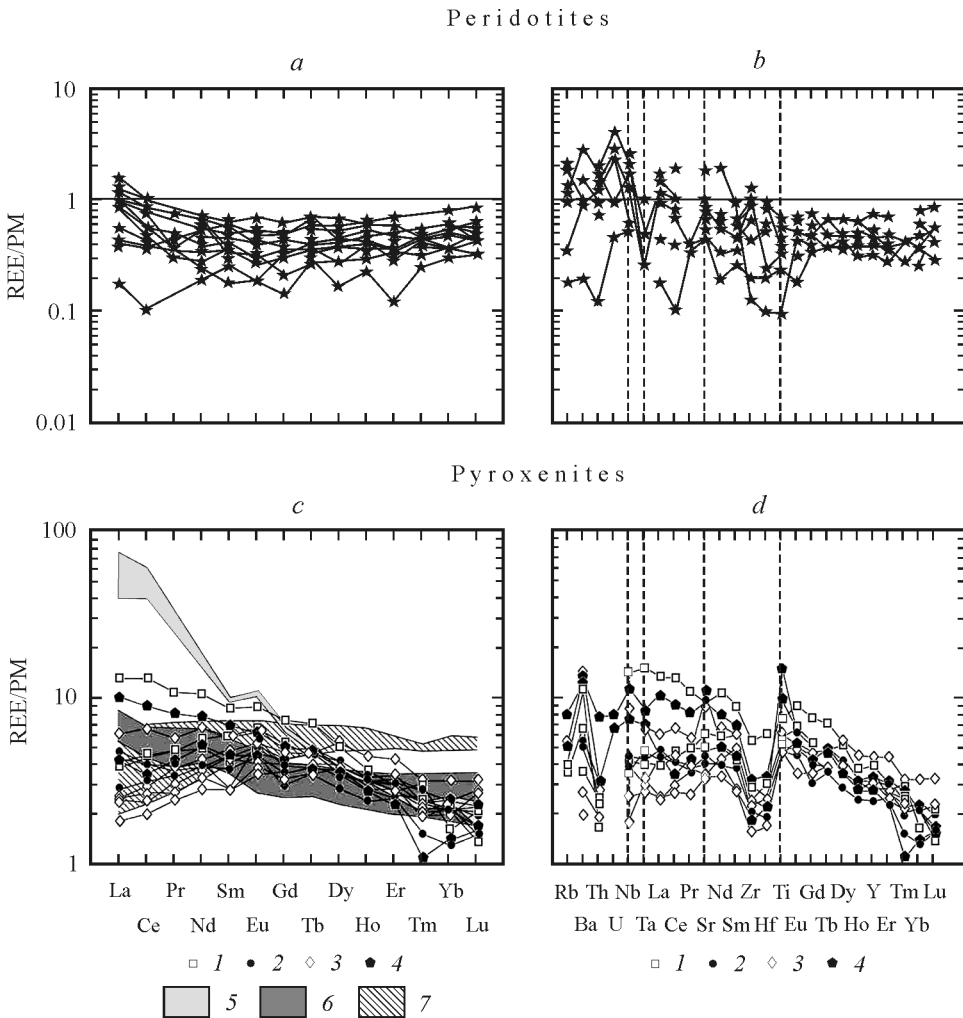


Fig. 2. Primitive mantle-normalized (Palme, O'Neill, 2003) trace elements distribution patterns for peridotite (up) (a, b) and pyroxenite (c, d) xenoliths (down). Shaded areas outline normalized patterns for different types of basalts.

1—4 — xenoliths: 1 — websterites, 2 — garnet websterites, 3 — garnet clinopyroxenites, 4 — amphibole-bearing garnet clinopyroxenites; 5 — alkaline olivine basalts of the Sverre and Halvdan volcanoes (Sushchevskaya et al., 2008); 6 — picrites (Zhang et al., 2008); 7 — MORB (Klein, 2003).

Рис. 2. Спектры редких элементов, нормированных к примитивной мантии (Palme, O'Neill, 2003) для ксенолитов перидотитов (вверху) и пироксенитов (внизу). Выделены области, соответствующие спектрам различных типов базальтов.

1998). The fields of pyroxenites are located separately on both plots, indicating differences between their compositions and those of main types of basalts (Fig. 1). Only websterites, as is seen on the Al/Si vs Mg/Si diagram, have compositions close to mid-ocean ridge tholeiites.

All of pyroxenites are enriched by REE relative to primitive mantle (Fig. 2, c). The mantle-normalized REE distribution patterns differ from those in the picrites (Zhang et al., 2008), N-MORB (Klein, 2003) and alkaline olivine basalts of Sverre and Halvdan volcanoes (Sushchevskaya et al., 2008).

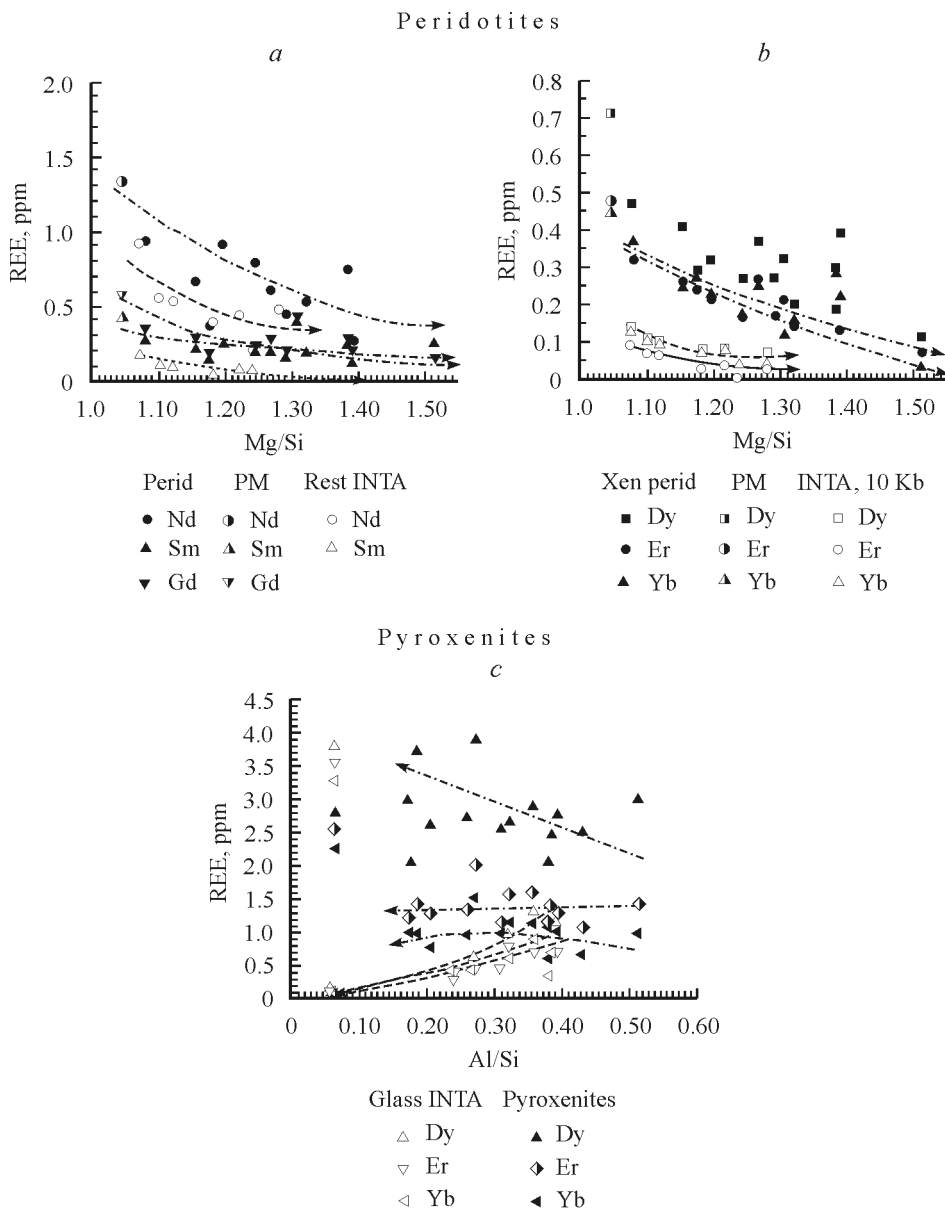


Fig. 3. REE concentrations vs Mg/Si (*a*, *b*) and Al/Si (*c*) ratios for xenoliths and products (restites and melts) of INTA spinel peridotite melting at 1270—1390 °C and 1/0 GPa (Schwab, Johnston, 2001). REE concentrations in primitive mantle (Palme, O'Neill, 2003) are also shown.

Рис. 3. Зависимости содержания REE от отношения Mg/Si и Al/Si в ксенолитах перидотитов и пироксенинтов, а также продуктах плавления (реститах и расплавах) шпинелевого перидотита INTA при 1270—1390 °C и 1.0 ГПа (Schwab, Johnston, 2001). Содержание элементов в примитивной мантии по: (Palme, O'Neill, 2003).

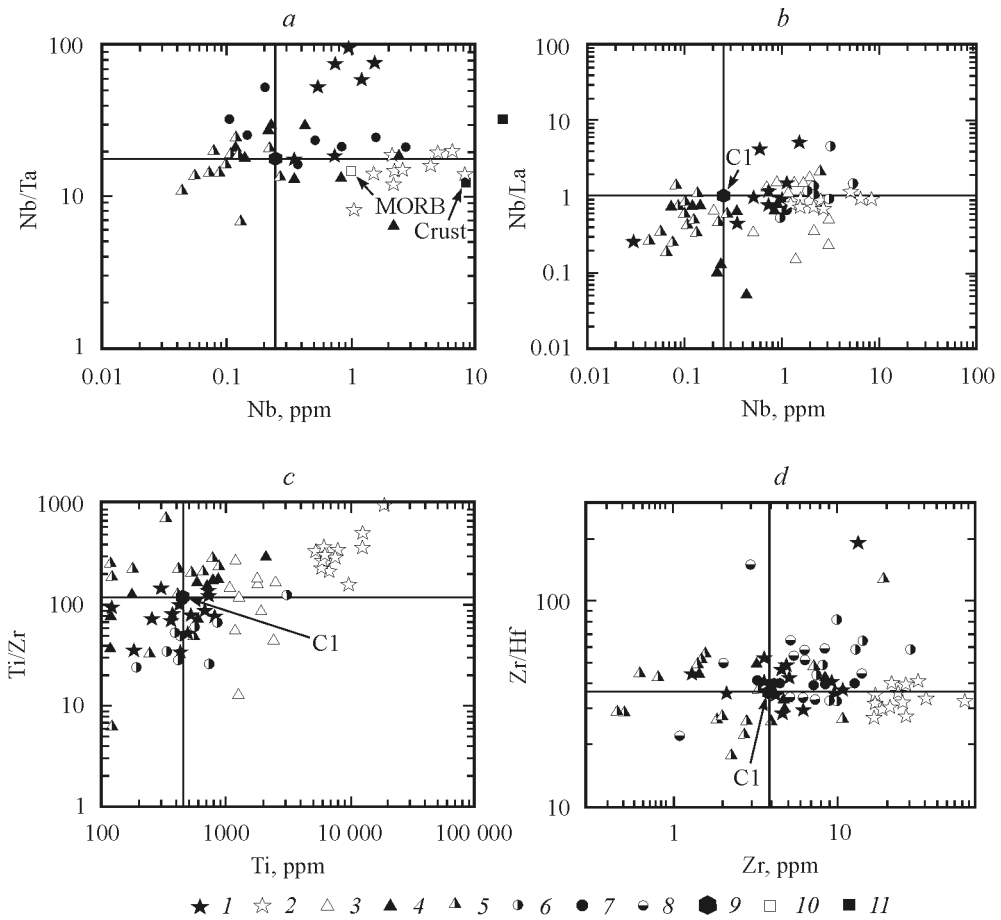


Fig. 4. Variation plots of HFS element concentrations vs their ratios for peridotite and pyroxenite xenoliths from Spitsbergen and other regions (a—d).

1, 2 — studied xenoliths; 1 — peridotites, 2 — pyroxenites; 3—8 — spinel peridotite xenoliths in Cenozoic basalts from the North China Craton; 3 — Hannuoba (Rudnick et al., 2004), 4, 5 — Wangoing and Longgoing (Wu et al., 2003), and from the Central Asian Folded Belt; 6 — Tokinsky Stanovik (A. Goncharov, personal communication), 7 — Barchatny eruption center (Kalfoun et al., 2002), 8 — Mongolia (Wiechert et al., 1997); 9 — chondrite C1 (Palme, O'Neill, 2003); 10 — MORB (Weyer et al., 2003); 11 — Earth's crust (Rudnick et al., 2000).

Рис. 4. Вариации содержаний HFS элементов и их отношений в ксенолитах перидотитов и пироксенитов из базальтов Шпицбергена и других регионов.

The dependences between REE concentrations and the Al/Si ratio in the pyroxenite xenoliths are not identical to those for melts experimentally formed in spinel Iherzolites at 1280—1390 °C and at 1.0 GPa (Johnston, Schwab, 2004). On Fig. 3, c, the trends of decrease in Dy, Er and Yb concentrations occupy a diagonal position relative to similar trends for the melts, in which concentrations of listed elements increase with the Al/Si ratio decreasing (this tendency is especially clear for Dy). Similar nonconformity also occurs for Zr, Y and Sr.

Positive anomalies for Ba and Ti, negative anomalies for Th, Zr, and Hf, and a weak positive anomaly for Sr are observed on the Rb-Lu PM-normalized plot (Fig. 2, d). The fields of pyroxenite and peridotite xenoliths are isolated on diagrams Nb/Ta vs Ta, Nb/La vs Nb, Ti/Zr vs Ti, and Zr/Hf vs Zr (Fig. 4). In case of pyroxenites, despite of a higher Nb content than in the peridotites, chondritic and

Table 3

Modal composition and $P-T$ conditions of mineral equilibria for pyroxenite xenoliths**Модальные составы и $P-T$ условия минеральных равновесий
для ксенолитов пикроксенитов**

Sample	Rock type	Modal composition, %					$T, ^\circ\text{C}$	P, GPa
		Amph	Cpx	Grt	Opx	Spl		
Sp-10	a	10	61	—	29	—	1010*	2.1
Sp-13	b	—	68	2	16	1	1310	3.3
Sp-14	a	—	65	—	31	4	1080*	2.3
Sp-16	c	—	53	47	—	—	—	—
Sp-18	c	5	52	33	—	10	—	—
Sp-19	c	—	61	37	—	2	—	—
Sp-21	c	—	71	22	—	7	—	—
Sp-22	c	6	54	16	22	2	1140	2.7
Sp-23	c	—	68	18	4	10	1100	2.2
Sp-26	a	—	—	—	—	—	1000*	2.1
Sp-36	c	—	—	—	—	—	—	—
Sp-4	c	—	65	33	4	—	1140	2.5

Notes. Rock type: a — websterite, b — garnet websterite, c — garnet clinopyroxenite. In case of garnet websterites, temperature and pressure calculated using the Grt-Opx thermobarometer (Nikitina et al., 2010); in case of garnet free pyroxenites, temperature calculated using the Opx-Cpx thermometer (Wood, Banno, 1973; indicated by an asterisk), pressure calculated by projection of temperature estimates to the 55 mW/m² regional geotherm of Hasterok and Chapman (2011).

sub-chondritic values of Nb/Ta (8.2—19.6) are predominantly observed, and the Nb/La ratio is usually less than in the chondrite C1 (Palme, O'Neill, 2003). These xenoliths are characterized by a significantly higher content of Ti (5400—18 700 ppm) in comparison with peridotites (60—780 ppm) and by a superchondritic Ti/Zr ratio. The Zr/Hf ratio varies from sub-chondritic to superchondritic (19.0—40.8), but sub-chondritic values predominate.

HFSE IN THE ROCK-FORMING MINERALS OF PERIDOTITE XENOLITHS

Trace elements contents in minerals of peridotite xenoliths are given in Table 5 and partition coefficients of HFSE between the coexisting minerals are in Table 6. Typical primitive mantle-normalized REE distribution patterns for Ol, Opx, and Cpx from peridotite sample 2166-25 (Fig. 5, a) show the maximum concentrations of REE in clinopyroxene and the minimum in olivine. The comparisons of sums of REE contents in xenoliths obtained by different ways (Fig. 5, b) reveal a close agreement among their values. These results provide an evidence that the major hosts for REE in spinel peridotites are rock-forming minerals: clinopyroxene, orthopyroxene and olivine. Among them, clinopyroxene has the highest contents of Nb, Ta, La, Zr, Hf, and Ti.

In spite of limited number of studied samples, there is possibility to analyse the effect of the temperature on the equilibrium distribution of HFSE between the minerals of spinel peridotites. The xenolith equilibrium temperatures and pressures span the ranges 730—1180 °C and 1.3—2.7 GPa, respectively. Peridotite xeno-

Table 4
Химический состав ксенолитов пироксенитов
Compositions of pyroxenite xenoliths (major oxides in wt %, trace elements in ppm)

Sample	Sp-10	Sp-14	Sp-32	Sp-13	Sp-16	Sp-19	Sp-4	Sp-21	Sp-22	Sp-23	Sp-25	Sp-11	Sp-18
SiO ₂	48.50	47.90	47.50	43.10	43.20	44.90	45.90	44.00	47.30	41.60	45.30	40.50	38.70
TiO ₂	1.23	1.10	1.57	1.02	0.99	0.98	1.29	0.99	0.88	2.09	1.02	3.12	2.04
Al ₂ O ₃	7.48	8.78	7.87	14.50	14.70	12.80	11.10	13.90	10.90	14.50	12.50	15.50	17.60
FeO	10.09	9.91	12.43	9.28	11.08	9.73	11.62	9.55	9.55	11.26	9.64	10.63	11.89
MnO	0.17	0.17	0.20	0.14	0.17	0.16	0.18	0.16	0.17	0.15	0.16	0.12	0.14
MgO	16.30	16.90	14.00	16.30	15.20	14.70	14.90	16.10	14.30	16.00	15.40	13.60	
CaO	13.50	12.30	12.50	13.40	11.80	14.10	12.50	14.40	12.80	12.90	13.20	11.10	12.90
Na ₂ O	1.38	1.42	2.19	1.32	1.24	1.19	1.33	1.17	1.26	1.51	1.19	1.83	1.60
K ₂ O	0.12	0.10	0.30	0.11	0.12	0.07	0.03	0.05	0.06	0.30	0.08	0.57	0.33
P ₂ O ₅	<0.05	<0.05	<0.05	<0.05	<0.05	<0.05	<0.05	<0.05	<0.05	<0.05	<0.05	<0.05	0.08
LOI	<0.1	-0.24	<0.1	<0.1	-0.24	<0.1	-0.10	<0.1	<0.1	-0.24	<0.1	<0.1	<0.1
Total	98.8	98.3	98.6	99.2	98.3	99.1	98.5	99.1	99.0	98.4	99.1	98.8	98.9
V	238	245	210	345	299	338	263	351	281	363	308	462	391
Cr	610	878	466	168	316	242	379	320	369	550	330	43.5	59.4
Co	57.30	54.30	57.50	73.00	77.50	71.40	69.30	75.30	58.90	72.60	69.00	80.10	85.10
Ni	78.70	76.90	42.60	71.00	34.90	38.50	50.60	40.30	52.80	51.00	39.90	30.60	27.50
Cu	71.40	45.00	45.30	52.00	28.90	64.80	54.30	59.10	61.80	49.90	67.20	44.30	30.50
Zn	59.40	91.90	103.00	91.60	87.00	59.80	96.10	65.10	115.00	71.70	87.80	131.00	
Ga	13.10	18.00	24.00	22.40	22.10	15.30	23.60	15.90	25.80	18.50	23.30	31.90	
Ge	1.65	1.16	1.79	1.41	1.44	1.61	1.57	1.49	1.50	1.56	1.29	1.24	1.14
Rb	2.14	<2	2.44	<2	<2	<2	<2	<2	<2	3.25	<2	3.08	4.80
Sr	121.00	97.50	186.00	88.40	79.30	70.00	70.40	64.00	61.30	174.00	67.90	216.00	187.00
Y	14.70	12.70	16.50	10.50	13.80	14.20	19.20	14.80	13.70	14.10	13.60	12.10	14.50
Zr	25.90	31.00	58.70	21.70	20.40	23.50	24.30	17.80	17.10	25.70	17.20	19.80	34.40
Nb	2.39	2.15	8.15	2.54	2.24	1.53	1.06	1.22	0.93	4.96	1.51	4.34	6.47
Mo	3.80	1.03	1.04	1.12	1.44	1.03	1.48	1.21	1.16	0.97	1.09	1.52	1.22
Sn	1.86	1.74	2.43	1.35	1.88	1.78	1.58	1.78	1.62	1.41	2.72	1.53	2.37

Table 4 (*continued*)

Sample	Sp-10	Sp-14	Sp-32	Sp-13	Sp-16	Sp-19	Sp-4	Sp-21	Sp-22	Sp-23	Sp-25	Sp-11	Sp-18
Sb	0.18	0.17	<0.1	0.15	0.16	0.15	0.27	0.17	0.13	0.16	0.17	0.17	0.14
Ba	44.40	24.00	74.20	34.10	36.60	18.50	13.50	15.30	12.60	95.80	18.20	93.20	82.20
Hf	0.94	0.76	1.79	0.56	0.67	0.76	0.58	0.62	0.66	0.52	0.66	0.66	1.01
Ta	0.16	0.18	0.58	0.17	0.12	<0.1	0.13	<0.1	<0.1	0.26	0.11	0.27	0.33
Pb	<1	<1	<1	<1	<1	<1	<1	<1	<1	<1	<1	<1	<1
Th	0.19	0.21	0.14	0.24	0.26	0.13	<0.1	0.18	<0.1	0.24	0.16	0.26	0.63
U	<0.1	<0.1	<0.1	<0.1	<0.1	<0.1	<0.1	<0.1	<0.1	<0.1	<0.1	<0.1	<1
La	2.71	2.89	8.92	3.25	2.99	1.97	1.72	1.69	1.24	4.17	1.74	2.93	6.96
Ce	7.88	8.07	23.30	7.21	7.23	5.52	5.30	4.31	3.63	11.60	4.83	6.07	15.90
Pr	1.30	1.32	2.91	0.99	1.05	0.93	1.02	0.83	0.66	1.55	0.72	1.15	2.16
Nd	7.56	6.61	14.00	5.15	5.46	5.14	5.61	4.93	3.75	8.84	4.49	6.75	10.30
Sm	2.58	1.79	3.72	1.61	1.22	1.94	2.11	1.87	1.22	2.57	1.22	1.93	2.85
Eu	1.06	0.77	1.44	0.73	0.88	0.73	0.86	0.66	0.63	1.02	0.57	0.84	1.00
Gd	3.01	2.42	4.25	1.75	2.25	2.04	2.70	2.32	1.87	2.85	2.03	2.46	2.85
Tb	0.49	0.38	0.74	0.37	0.40	0.40	0.49	0.42	0.37	0.50	0.40	0.50	0.52
Dy	2.98	2.61	3.72	2.04	2.45	2.64	3.87	2.87	2.75	2.75	2.75	2.49	2.97
Ho	0.52	0.46	0.58	0.39	0.50	0.48	0.72	0.54	0.45	0.52	0.45	0.44	0.52
Er	1.24	1.30	1.42	1.15	1.40	1.56	2.02	1.60	1.34	1.30	1.16	1.07	1.43
Tm	0.18	0.22	0.17	0.11	0.14	0.20	0.23	0.17	0.14	0.16	0.15	0.08	0.20
Yb	0.99	0.76	0.97	0.61	1.05	1.13	1.50	1.14	0.94	1.01	0.98	0.67	0.98
Lu	0.15	0.15	0.10	0.11	0.14	0.16	0.23	0.20	0.19	0.11	0.16	0.11	0.12
Nb/Ta	14.94	11.94	14.05	14.94	18.67	—	8.15	—	—	19.08	13.73	16.07	19.61
Nb/La	0.88	0.74	0.91	0.78	0.75	0.78	0.62	0.72	0.75	1.19	0.87	1.48	0.93
Ti/Zr	284.47	212.55	160.21	281.56	290.69	249.80	317.99	333.15	308.26	487.12	355.22	943.88	355.22
Zr/Hf	27.55	40.79	32.79	38.75	30.45	35.07	31.97	30.69	27.58	38.94	33.08	30.00	34.06

Trace element contents (ppm)
Содержание редких элементов (ppm)

Sample	2162-2			2166-3			2166-8		
	Mineral	Ol	Opx	Cpx	Ol	Opx	Cpx	Ol	Opx
Mode, %	74	16	8	52	29	15	79	10	8
T, °C		1060			910			770	
F, %		29			0			27	
La	0.003	0.01	11.7	0.002	0.011	0.628	0.052	0.006	4.06
Ce	0.016	0.066	37.4	0.007	0.043	3.97	0.177	0.04	7.32
Pr	—	0.013	4.81	—	0.009	0.766	0.014	0.006	0.855
ZNd	—	0.093	23.9	—	0.106	5.38	0.02	0.029	5.32
Sm	0.007	0.039	4.84	—	0.039	2.57	0.014	0.02	2.03
Eu	0.002	0.015	1.6	—	0.011	0.974	0.004	0.01	0.814
Gd	0.004	0.049	3.08	—	0.049	3.17	0.018	0.03	3.45
Dy	—	0.07	2.48	0.015	0.124	4.18	0.01	0.1	3.86
Er	—	0.094	1.44	—	0.101	2.71	0.004	0.198	2.59
Yb	0.012	0.188	1.42	—	0.237	2.49	0.019	0.305	2.8
Ti	15.61	130	478	17.1	850	4108	17	592	3088
V	9.36	73.1	171	10	112	265	11.6	109	276
Cr	0.503	2158	4424	78	1685	3801	161	1959	4719
Sr	276	0.44	304	0.582	0.488	47.4	1.46	0.514	75.8
Y	0.043	0.615	11.6	0.041	0.868	22.8	0.152	0.89	21.7
Zr	0.363	0.424	10.1	0.12	1.28	34.9	0.184	1.06	31.1
Nb	0.004	0.018	0.499	0.01	0.005	0.22	0.006	0.011	0.159
Ba	0.137	0.056	3.69	0.188	0.051	0.371	0.56	0.113	0.653
Hf	—	0.027	0.531	—	0.042	1.47	—	0.047	1.49
Ta	—	0	0.149	—	0.014	0.281	—	0.014	0.254
U	—	0.003	4.03	—	0.003	0.004	—	0.012	0.2
Nb/Ta	—	—	3.35	—	0.36	0.78	—	0.79	0.63
Nb/La	1.33	1.80	0.04	5.00	0.46	0.35	0.12	1.83	0.04
Ti/Zr	43.00	306.60	47.33	142.50	664.06	117.71	92.39	558.49	99.29
Zr/Hf	—	15.70	19.02	—	30.48	23.74	—	22.55	20.87

liths, for which trace elements in minerals were determined, mostly are assembled from basalts of the Sverre volcano. The xenoliths from volcanoes Sigurd (sample 2166-2) and Halvdan (sample 2166-24) were excluded from the examination, since they are considerably different in trace element contents and their ratios from the xenoliths of the Sverre volcano.

In clinopyroxenes from peridotite xenoliths of the Sverre volcano, the temperature dependence of Nb concentrations are positive, whereas this dependence for Ta, Zr and Hf are weak or absent. The positive temperature dependences are also observed for Nb and Ta in orthopyroxenes (Table 7). The temperatures dependences of Ti content in both pyroxenes are not clear, although a positive dependence of this kind is observed distinctly in olivine. The Ti/Zr ratio in both pyroxenes increases with an increase in temperature. The Nb/Ta ratio in orthopyroxene decreases when temperature increases, while in clinopyroxene it increases at the same time. The

Table 5

in minerals of spinel peridotites

в минералах шпинелевых перидотитов

2166-9			2166-10			2166-11	
Opx	Cpx	Ol	Opx	Cpx	Ol	Opx	Cpx
23	11	59	27	12	78	10	9
850			730			1030	
15			10			30	
0.015	6.91	0.008	—	2.38	0.004	—	1.76
0.038	12.4	0.029	0.007	4.09	0.018	0.02	4.37
—	1.33	0.002	—	0.657	0.002	—	0.745
0.03	6.99	0.014	0.005	5.02	0.006	0.013	7.27
0.008	2.11	0.006	0.008	2.4	0.01	—	2.37
0.006	0.745	0.007	0.006	0.997	—	—	1.06
0.044	2.22	0.007	0.033	3.18	—	0.025	2.96
0.114	3.16	0.007	0.077	3.99	—	0.08	4.54
0.124	2.15	0.004	0.107	3.42	0.004	0.076	2.84
0.255	2.09	0.018	0.207	3.15	0.006	0.172	2.58
388	1889	10.9	680	3943	12.9	569	5868
91.3	249	10.8	98.5	280	11.8	90.9	464
1666	3672	156	1676	4259	187	1926	5151
0.203	77.1	0.711	0.135	65	1.08	0.167	58.6
0.748	17.3	0.031	0.626	22.2	0.042	0.613	34.4
0.794	21	0.263	1.18	37.7	0.273	0.897	31.4
0.01	0.149	0.008	0.004	0.149	0.009	0.008	1.3
0.043	0.166	2.75	0.041	1.83	0.196	0.055	1.12
0.058	0.981	—	0.017	1.76	—	0.019	1.37
0.02	0.187	—	0.005	0.349	—	0.011	0.274
0.016	0.184	—	0.003	1.65	—	0.014	0.074
0.50	0.80	—	0.80	0.43	—	0.73	4.75
0.67	0.02	1.00	—	0.06	2.25	—	0.74
488.67	89.95	41.45	576.27	104.59	47.25	634.34	186.88
13.69	21.41	—	69.41	21.42	—	47.21	22.92

partition coefficients D_{Ti} in mineral pairs orthopyroxene-clinopyroxene, olivine—clinopyroxene, olivine—orthopyroxene increase with an increase in temperature (Table 7). $D_{\text{Opx}-\text{Cpx}}^{\text{Opx}-\text{Cpx}}$ is considerably higher (>0.1) than $D_{\text{Ti}}^{\text{Ol}-\text{Cpx}}$ (<0.1) and $D_{\text{Ti}}^{\text{Ol}-\text{Opx}}$ (<0.01). $D_{\text{Nb}}^{\text{Opx}-\text{Cpx}}$ and $D_{\text{Ta}}^{\text{Opx}-\text{Cpx}}$ both reveal significant temperature dependences: the first decreases, and the second increases with an increase in temperature.

DISCUSSION

The partition of HFSE between minerals and fractionation of these elements in spinel peridotites in the continental lithospheric mantle beneath north-west Spitsbergen require discussion. Peridotites are melting residues of a substratum, that is close to primitive mantle, and represent the mantle depleted by main lithophile

Table 5 (continued)

Sample	2166-18			2166-24			2166-25		
Mineral	OI	Opx	Cpx	OI	Opx	Cpx	OI	Opx	Cpx
Mode, %	69	18	10	60	27	10	67	21	10
T, °C		930			880			1150	
F, %		24			13			22	
La	0.003	—	6.21	0.003	0.007	3.54	0.007	0.017	11.6
Ce	0.03	0.027	11.9	0.033	0.012	3.83	0.019	0.066	19.6
Pr	0.003	—	1.3	0.001	—	0.228	0.004	0.013	—
Nd	0.01	0.028	6.94	0.007	0.018	1.3	0.023	0.066	10.09
Sm	—	0.02	2.3	—	—	1.16	0.013	0.032	2.54
Eu	0.003	0.012	0.927	—	0.007	0.432	0.009	0.014	0.864
Gd	0.002	0.107	3.05	0.003	0.022	2.15	0.014	0.034	2.81
Dy	0.003	0.09	3.84	0.003	0.048	2.96	—	0.091	3.06
Er	—	0.389	2.72	—	0.106	2.23	0.022	0.138	1.86
Yb	0.019	0.026	2.55	0.018	0.163	2.43	0.041	0.218	1.59
Ti	18.5	687	4197	12.6	382	1742	26.5	601	2703
V	13.7	98.3	325	11.7	85.6	231	110	90.8	244
Cr	228	1869	7667	174	1451	3437	0.557	2287	4577
Sr	0.545	0.298	123	0.592	0.154	61	302	0.375	174
Y	0.059	0.871	22.9	0.05	0.605	16.4	0.07	0.933	18
Zr	0.211	1.22	41.3	0.253	0.3	6.65	0.564	2.69	48.4
Nb	0.005	0.026	0.229	0.005	0.01	0.161	0.072	0.013	0.684
Ba	0.071	0.106	0.252	0.242	0.043	1.35	0.199	0.102	0.434
Hf	—	0.061	1.81	—	0.023	0.828	—	0.061	1.5
Ta	—	0.02	0.269	—	0.008	0.229	—	0.038	0.254
U	—	0	0.133	—	0.007	0.147	—	0.008	0.189
Nb/Ta	—	1.30	0.85	—	1.25	0.70	—	0.34	2.69
Nb/La	1.67	—	0.04	1.67	1.43	0.05	10.29	0.77	0.06
Ti/Zr	87.68	563.12	101.62	49.80	1273.33	261.96	46.99	223.42	55.85
Zr/Hf	—	20.00	22.82	—	13.04	8.03	—	44.10	32.27

components (Al_2O_3 , CaO , and FeO) and trace elements (V, Sr, Y, Ti, Zr, Nb, Ta, and REE). These rocks have been crystallized at the deep level close to the boundary of the phase transition of spinel peridotites into garnet peridotites in $\text{CaO}-\text{MgO}-\text{Al}_2\text{O}_3$ system at 730–1180 °C, 1.3–2.7 GPa. Both Zr/Hf and Nb/Ta ratios in peridotites vary from sub-chondritic to superchondritic, whereas in pyroxenites, as in basalts, the Nb/Ta ratio is predominantly sub-chondritic (8.2–19.6). The Nb/La ratio in pyroxenites are also usually lower than chondritic. Additionally, sub-chondritic values of Zr/Hf are established for the majority of pyroxenite xenoliths.

The distribution of trace elements between olivine, orthopyroxene and clinopyroxene in spinel peridotites and temperature dependences of partition coefficients were studied experimentally at 1150–1500 K and 1.5 GPa (Witt-Eickschen, O'Neill, 2005). It was shown that HFSE are redistributed from clinopyroxene into orthopyroxene with an increase in temperature. The last mineral and olivine also can be the main carriers of many incompatible rare elements at magmatic tempera-

Table 6

The Ti, Zr, Nb, Ta partition coefficients between the minerals of the spinel peridotite xenoliths (the Sverre volcano)

Коэффициенты распределения Ti, Zr, Nb, Та между минералами ксенолитов шпинелевых перидотитов (вулкан Сверре)

Sample	$T, ^\circ\text{C}$	$D^{\text{Opx-Cpx}}$					$D^{\text{Ol-Opx}}$			$D^{\text{Ol-Cpx}}$		
		Ti	Zr	Nb	Hf	Ta	Ti	Zr	Nb	Ti	Zr	Nb
2166-2	1060	0.272	0.042	0.036	0.051	—	0.012	0.036	0.008	0.033	0.856	0.222
2166-3	910	0.207	0.037	0.041	0.029	0.050	0.004	0.003	0.082	0.020	0.094	2.000
2166-8	770	0.192	0.034	0.069	0.032	0.055	0.006	0.006	0.038	0.29	0.174	0.546
2166-9	850	0.205	0.038	0.067	0.059	0.107	—	—	—	—	—	—
2166-10	730	0.173	0.031	0.027	0.010	0.014	0.003	0.007	0.054	0.016	0.223	2.000
2166-18	930	0.164	0.030	0.114	0.034	0.074	0.008	0.003	0.005	0.027	0.173	0.192
2166-24	880	0.219	0.045	0.062	0.028	0.035	0.007	0.038	0.031	0.033	0.843	0.500
2166-25	1150	0.222	0.056	0.048	0.041	0.150	0.010	0.012	0.105	0.044	0.210	2.182

tures. The data obtained in the present work regarding the partition of HFSE between the minerals of spinel lherzolites and temperature dependences of trace element content and their ratios agree with the experimental data. There are temperature dependences of Nb and Ta contents in clinopyroxene and orthopyroxene from spinel peridotites over the range of 700—1200 °C. The Nb content and the Nb/Ta ratio in clinopyroxenes increase with an increase in temperature. The Nb and Ta content in othopyroxenes increase when temperature increases, whereas the Nb/Ta ratio dec-

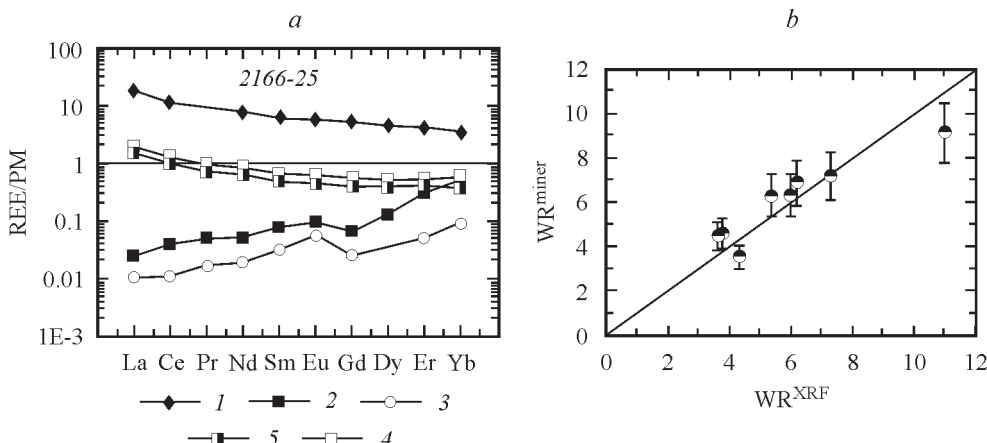


Fig. 5. Mantle-normalized REE distribution patterns for peridotite sample 2166-25 (a) and the plot of comparison of the sum of REE contents in studied peridotites obtained by the XRF method (WR^{XRF}) and the same sum calculated from REE contents in olivine, orthopyroxene and clinopyroxene ($WR^{mineral}$), based on mineral modes in xenoliths (b).

When calculating WR^{XRF} and $WR^{mineral}$, Tb, Ho, Tm, and Lu are ignored because these elements are not detected in studied minerals. 1 — clinopyroxene, 2 — orthopyroxene, 3 — olivine, 4 — $WR^{mineral}$, 5 — WR^{XRF} .

Fig. 5. Нормированное к примитивной мантии распределение редкоземельных элементов в образце пе-риодита 2166-25 (a) и график сравнения суммы содержаний REE в перидотитах, определенных ме-тодом RRF и рассчитанных на основе данных о содержании редкоземельных элементов в оливине, орто-пиroxене и клинопироксене и модального содержания минералов в ксенолитах (b).

Table 7

Parameters of linear temperature dependence of Ti, Nb, Ta, Zr, Hf contents, their ratios in minerals, and their partition coefficients between minerals of spinel peridotite xenoliths (the Sverre volcano)

Параметры линейной температурной зависимости содержаний Ti, Nb, Ta, Zr, Hf, их отношений в минералах и коэффициентов распределения элементов между минералами в ксенолитах шпинелевых перидотитов (вулкан Сверре)

Linear equation $y = a + bT$	a	$b \cdot 10^4$	r^2	n
Element content in minerals				
Nb ^{Opx}	-0.0384	6	0.793	8
Nb ^{Cpx}	-0.932	13.2	0.89	8
Ta ^{Opx}	-0.0045	0.7	0.879	8
Zr ^{Olx}	-0.388	7.2	0.74	7
Element ratio in minerals				
Ti/Zr ^{Cpx}	185.14	-1070	0.891	5
Ti/Zr ^{Opx}	1219.7	-8382	0.916	7
Nb/Ta ^{Cpx}	-3.622	52	0.9	5
Nb/Ta ^{Opx}	1.565	-11	0.84	5
Partition coefficients of element between minerals				
D _{Ti} ^{Opx-Cpx}	0.704	1.6	0.766	6
D _{Ti} ^{Olx-Opx}	-0.009	0.2	0.823	7
D _{Ti} ^{Olx-Cpx}	-0.024	0.6	0.821	7
D _{Nb} ^{Opx-Cpx}	0.122	-0.7	0.728	6
D _{Ta} ^{Opx-Cpx}	-0.173	2.7	0.803	7

Notes. T is the temperature in degrees of Celsius, r^2 is a coefficient of correlation, n is a number of samples.

reases. No distinct temperature dependences of Ti contents in orthopyroxene and clinopyroxene are observed in studied rocks, whereas olivine is somewhat enriched with this element. Taking into account that peridotites have high modal content of olivine and this content increases as partial melting increases, olivine may be considered as a main concentrator of Ti in harzburgites and dunites. The partition coefficients of Ti between olivine and orthopyroxene and between olivine and clinopyroxene increase with an increase in temperature. Likewise, $D_{Ti}^{Opx-Cpx}$ are positively related with temperature. The values of $D_{Nb}^{Opx-Cpx}$ and $D_{Ta}^{Opx-Cpx}$ correlate with temperature, too. It is indicated that redistribution of Ta between orthopyroxene and clinopyroxene occurs with increasing temperature from 700 to 1200 °C: orthopyroxene concentrates Ta, while clinopyroxene is enriched with Nb. Based on these data, we can draw some overall conclusions relative to fractionation of Nb, Ta, Zr, Hf, and Ti between rock-forming minerals at the temperature from 700 to 1200 °C and comparably low pressure.

It is clear that the partial melting regulates HFSE fractionation in the mantle, because of the temperature and pressure dependence of partition coefficients of these elements between minerals and melts (Foley et al., 2000). Thermodynamic conditions for melting as well as chemical compositions of minerals determine the de-

gree of fractionation. It is possible to conclude that the process of Nb, Ta, Zr, and Ti fractionation occurs already in the upper part of the continental lithospheric mantle under conditions that exist at depth corresponding to the Moho discontinuity (the boundary of the phase transition of spinel peridotites into garnet peridotites in CMAS system). However, the degree of fractionation of HFSE elements in mantle rocks of north-west Spitsbergen is noticeably weaker than in the mantle beneath Early Precambrian cratons (Nikitina et al., 2014; Nikitina et al., 2015), i.e., at higher temperature and pressure (in the conditions of the diamond depth facies).

CONCLUSION

Our study of mantle xenoliths from Quaternary volcanoes of north-west Spitsbergen have led to the conclusion, that fractionation of Nb, Ta, Zr, Hf, and Ti occurs in the upper part of the continental lithospheric mantle under the conditions that exist at depth corresponding to the Moho discontinuity. These conditions correspond to those of the phase transition of spinel peridotites into garnet peridotites in the CMAS systems. It is most likely that the degree of partial melting and the thermodynamic conditions of this process are the main factors regulating fractionation of HFSE. The fractionation of these elements in the mantle of north-west Spitsbergen is noticeably different than in the mantle beneath Early Precambrian cratons.

Acknowledgements. This research was supported by the Russian Foundation for Basic Research (RFBR), projects No.10-05-01017, No.11-05-00346, and by a grant from the President RF NSH-5710.2010.5.

References

- Amundsen H. E. F., Griffin W. L., O'Reilly S. Y. The lower crust and upper mantle beneath north-western Spitsbergen: evidence from xenoliths and geophysics. *Tectonophysics*. **1987**. Vol. 139. P. 169—185.
- Barth M. G., McDonough W. F., Rudnick R. L. Tracking the budget of Nb and Ta in the continental crust. *Chem. Geol.* **2000**. Vol. 165. P. 197—213.
- Büchl A., Brügmann G., Batanova V. G., Munker C., Hofmann A. W. Melt percolation monitored by Os isotopes and HSE abundances: a case study from the mantle section of the Troodos Ophiolite. *Earth Planet. Sci. Lett.* **2002**. Vol. 204. P. 385—402.
- Evdokimov A. N. Volcanoes of Spitsbergen. St. Petersburg: VNIOkeangeologija, **2000**. 123 p. (*in Russian*).
- Farmer G. L. Continental Basaltic Rocks. In: Treatise on Geochemistry. Ed. by Holland H. D., Turekian K. K. Oxford: Pergamon Press, **2003**. Vol. 3.03. P. 1—39.
- Fedotova A. A., Bibikova E. V., Simakin S. G. Ion-microprobe zircon geochemistry as an indicator of mineral genesis during geochronological studies. *Geochem. Int.* **2008**. Vol. 46. P. 912—927.
- Foley S. F., Barth M. G., Jenner G. A. Rutile/melt partition coefficients for trace elements and an assessment of the influence of rutile on the trace element characteristics of subduction zone magmas. *Geochim. Cosmochim. Acta*. **2000**. Vol. 64. P. 933—938.
- Genshaft Y. S., Ilupin I. P. Mineralogy of Quaternary volcanic rocks from Spitsbergen. *Doklady Acad. Sci. USSR*. **1987**. Vol. 295. P. 168—173.
- Genshaft Y. S., Dashevskaya D. M., Evdokimov A. N., Kopylova M. G. Prevalence, shape and distribution of deep inclusions in basalts SW Spitsbergen. *Doklady Acad. Sci. USSR*. **1993**. Vol. 325. N 3. P. 565—571 (*in Russian*).
- Glebovitskii V. A., Nikitina L. P., Goncharov A. G., Borovkov N. V., Sirotkin A. N. Depleted and enriched matter in the upper mantle of Spitsbergen: Evidence from the study of mantle xenoliths. *Doklady Earth Sci.* **2011**. Vol. 439. P. 1016—1020.
- Goncharov A. G., Nikitina L. P., Babushkina M. S., Borovkov N. V., Sirotkin A. N. Petrology of mantle xenoliths from basalts of Spitsbergen: the age and formation conditions. In: Abst. XII Russian

petrograph. meeting «Petrography of igneous and metamorphic rocks» Petrozavodsk, 15—20 September 2015.

Hasterok D., Chapman D. S. Heat production and geotherms for the continental lithosphere. *Earth Planet. Sci. Lett.* **2011**. Vol. 307. P. 59—70.

Ionov D. A., Dupuy C., O'Reilly S. Y., Kopylova M. G., Genshaft Y. S. Carbonated peridotite xenoliths from Spitsbergen: implications for trace element signature of mantle carbonate metasomatism. *Earth Planet. Sci. Lett.* **1993**. Vol. 119. P. 283—297.

Ionov D. A., O'Reilly S. Y., Kopylova M. G., Genshaft Y. S. Carbonate-bearing mantle peridotite xenoliths from Spitsbergen: phase relationships, mineral compositions and trace element residence. *Contrib. Miner. Petrol.* **1996**. Vol. 125. P. 375—392.

Jagoutz E., Palme H., Baddehausen H., Blum K., Cendales M., Dreibus G., Spettel B., Lorenz V., Wänke H. The abundances of major, minor and trace elements in the Earth's mantle as derived from primitive ultramafic nodules. *Geochim. Cosmochim. Acta supplement.* **1979**. Vol. 11. N 2 (Proc. Lunar Planet. Sci. Conf. 10th). P. 2031—2050.

Johansson A., Gee D. G., Larionov A. N., Ohta Y., Tebenkov A. M. Grenvillian and Caledonian evolution of eastern Svalbard — a tale of two orogenies. *Terra Nova.* **2005**. Vol. 17. P. 317—325.

Johnston A. D., Schwab B. E. Constraints on clinopyroxene/melt partitioning of REE, Rb, Sr, Ti, Cr, Zr, and Nb during mantle melting: First insights from direct peridotite melting experiments at 1.0 GPa. *Geochim. Cosmochim. Acta.* **2004**. Vol. 68. P. 4949—4962.

Kalfoun F., Ionov D., Merlet C. HFSE residence and Nb-Ta ratios in metasomatized, rutile-bearing mantle peridotites. *Earth Planet. Sci. Lett.* **2002**. Vol. 199. P. 49—65.

Klein E. M. Geochemistry of the igneous oceanic crust. In: Treatise on Geochemistry. Ed. by Holland H.D., Turekian K.K. Oxford: Pergamon Press, **2003**. Vol. 3.13 P. 433—463.

König S., Schuth S. Deep melting of old subducted oceanic crust recorded by superchondritic Nb/Ta in modern island arc lavas. *Earth Planet. Sci. Lett.* **2011**. Vol. 301. P. 265—274.

Kopylova M. G., Genshaft Y. S., Dashevskaya D. M. Petrology of upper mantle and lower crustal xenoliths from the North-Western Spitsbergen. *Petrology.* **1996**. Vol. 4. P. 493—518.

Mann U., Frost D. J., Rubie D. C. Evidence for high-pressure core-mantle differentiation from the metal-silicate partitioning of lithophile and weakly-siderophile elements. *Geochim. Cosmochim. Acta.* **2009**. Vol. 73. P. 7360—7386.

Maslov V. A. Mantle inclusions in alkaline basaltoid of Sverre volcano, archipelago Spitsbergen: petrography, geochemistry, platiniferous rocks. PhD thesis syn. Saint Petersburg: Mining University, **2000**. 28 p.

Maslov V. A., Lasarenkov V. G. Structure types of mantle xenoliths from Sverre volcano basanites (Spitsbergen). *Proc. High Schoos. Geol. Explor.* **1999**. Vol. 6. 45—52 (in Russian).

Münker C., Pfänder J. A., Weyer S., Büchl A., Kleine T., Mezger K. Evolution of planetary cores and the Earth-Moon system from Nb/Ta systematics. *Science.* **2003**. Vol. 301. P. 84—87.

Nikitina L. P., Babushkina M. S., Korolev N. M., Goncharov A. G. HFSE in the continental lithospheric mantle: conditions and mechanism of fractionation (data of mantle xenoliths). Proc. XII All-Russian Conference «Petrography of magmatic and metamorphic rocks». St. Petrozavodsk, **2015**. P. 203—205.

Nikitina L. P., Korolev N. M. Fractionation of Nb, Ta, Zr, and Hf in continental lithospheric mantle (mantle xenoliths data). Proc. XIII Intern. Conference «Physicochemical and petrophysical investigations in Earth Sciences». Moscow, **2013**. P. 202—205.

Nikitina L., Goncharov A., Saltykova A., Babushkina M. The redox state of the continental lithospheric mantle of the Baikal-Mongolia region. *Geochem. Int.* **2010**. Vol. 48. P. 15—40.

Nikitina L. P., Korolev N. M., Zinchenko V. N., Felix J. T. Eclogites from the upper mantle beneath the Kasai Craton (Western Africa): Petrography, whole-rock geochemistry and UPb zircon age. *Precambrian Res.* **2014**. Vol. 249. P. 13—32.

Palme H., O'Neill H. S. C. Cosmochemical estimates of mantle composition. In: Treatise on Geochemistry. Ed. by Holland H.D., Turekian K.K. Oxford: Pergamon Press, **2003**. Vol. 2. The Mantle and Core. P. 1—38.

Pfänder J. A., Münker C., Stracke A., Mezger K. Nb/Ta and Zr/Hf in ocean island basalts — Implications for crust-mantle differentiation and the fate of niobium. *Earth Planet. Sci. Lett.* **2007**. Vol. 254. P. 158—172.

Pfänder J. A., Jung S., Münker C., Stracke A., Mezger K. A possible high Nb/Ta reservoir in the continental lithospheric mantle and consequences on the global Nb budget — Evidence from continental basalts from Central Germany. *Geochim. Cosmochim. Acta.* **2012**. Vol. 77. P. 232—251.

Rudnick R. L., Barth M., Horn I., McDonough W. F. Rutile-bearing refractory eclogites: missing link between continents and depleted mantle. *Science.* **2000**. Vol. 287. P. 278—281.

- Rudnick R. L., Gao S., Ling W.-L., Liu Y.-S., McDonough W. F. Petrology and geochemistry of spinel peridotite xenoliths from Hannuoba and Qixia. North China craton. *Lithos*. **2004**. Vol. 77. P. 609—637.
- Schmidt A., Weyer S., John T., Brey G. P. HFSE systematics of rutile-bearing eclogites: New insights into subduction zone processes and implications for the earth's HFSE budget. *Geochim. Cosmochim. Acta*. **2009**. Vol. 73. P. 455—468.
- Schwab B. E., Johnston A. D. Melting systematics of modally variable, compositionally intermediate peridotites and the effects of mineral fertility. *J. Petrol.* **2001**. Vol. 42. P. 1789—1811.
- Shubina N. A., Ukhakov A. V., Genshaft Y. S., Kolesov G. M. Trace and major elements in peridotites beneath North Western Spitsbergen — a contribution to the problem of mantle heterogeneity. *Geochem.* **1997**. N 1. P. 21—36 (in Russian).
- Sirokin A. N., Sharin V. V. Age of manifestation of Quaternary volcanism in Bjckfjorden (Spitsbergen Archipelago). *Geomorphology*. **2000**. Vol. 1. P. 95—105 (in Russian).
- Sushchevskaya N. M., Evdokimov A. N., Belyatsky B. V., Maslov V. A., Kuz'min D. V. Conditions of Quaternary magmatism at Spitsbergen Island. *Geochem. Int.* **2008**. N 46. P. 1—16.
- Wade J., Wood B. J. The Earth's 'missing' niobium may be in the core. *Nature*. **2001**. Vol. 409. P. 75—78.
- Walter M. J. Melting of garnet peridotite and the origin of komatiite and depleted lithosphere. *J. Petrol.* **1998**. Vol. 39. P. 29—60.
- Weyer S., Münker C., Mezger K. Nb/Ta, Zr/Hf and REE in the depleted mantle: implications for the differentiation history of the crust-mantle system. *Earth Planet. Sci. Lett.* **2003**. Vol. 205. P. 309—324.
- Wiechert U., Ionov D. A., Wedepohl K. H. Spinel peridotite xenoliths from the Atsagin-Dush volcano. Dariganga lava plateau. Mongolia: A record of partial melting and cryptic metasomatism in the upper mantle. *Contrib. Miner. Petrol.* **1997**. Vol. 126. P. 345—364.
- Witt-Eickschen G., O'Neill H. S. C. The effect of temperature on the equilibrium distribution of trace elements between clinopyroxene, orthopyroxene, olivine and spinel in upper mantle peridotite. *Chem. Geol.* **2005**. Vol. 221. P. 65—101.
- Wood B. J., Banno S. Garnet-orthopyroxene and orthopyroxene-clinopyroxene relationships in simple and complex systems. *Contrib. Miner. Petrol.* **1973**. Vol. 42. P. 109—124.
- Wu F., Walker R. J., Ren X., Sun D., Zhou X. Osmium isotopic constraints on the age of lithospheric mantle beneath northeastern China. *Chem. Geol.* **2003**. Vol. 196. P. 107—129.
- Zhang Z., Mao J., Cai J., Kusky T. M., Zhou G., Yan S., Zhao L. Geochemistry of picrites and associated lavas of a Devonian island arc in the northern Junggar terrane. Xinjiang (NW China): Implications for petrogenesis, arc mantle sources and tectonic setting. *Lithos*. **2008**. Vol. 105. P. 379—395.

Поступила в редакцию
16 июня 2015 г.